Enhanced Photostability of the Anthracene Chromophore in Aqueous Medium upon Protein Encapsulation

Rafael Alonso, Minoru Yamaji,† M. Consuelo Jiménez,* and Miguel A. Miranda*

Departamento de Química/Instituto de Tecnología Química UPV-CSIC, Universidad Politécnica de Valencia, Camino de Vera s/n, E-46022 Valencia, Spain

Received: May 28, 2010; Revised Manuscript Received: July 21, 2010

In the present work, 9-anthraceneacetic acid (**1**) has been selected as a simple, water-compatible derivative of the anthracene chromophore to investigate the photophysical and photochemical behavior upon binding to human and bovine serum albumins (HSA and BSA) and α-acid glycoproteins (HAAG and BAAG). The UV−vis absorption spectrum of **1** exhibited the typical four maxima between 320 and 400 nm, which were slightly red-shifted in the presence of proteins. These minor changes suggested the formation of **1**@protein complexes; their stoichiometry (1:1) was determined by means of the corresponding Job plots. As expected, the fluorescence spectrum of **1** in phosphate-buffered saline (PBS) consisted of a structured emission with maxima between 390 and 470 nm. The addition of increasing amounts of HSA resulted in a decrease in the emission intensity. In the presence of BSA, HAAG, or BAAG, the same trend was observed, although the changes were less pronounced. The determination of binding constants was achieved from fluorescence titration, considering one (AAGs) or two (SAs) binding sites. The binding constants (K_B) were found to be 2.3×10^6 M^{-1} (HAAG), 2.4×10^6 M^{-1} (BAAG), $4.57 \times 10^4/1.45 \times 10^6$ M^{-1} (HSA), and $1.44 \times 10^4/1.20 \times 10^6$ M^{-1} (BSA). Binding within two different sites of SAs was confirmed by displacement experiments using warfarin and ibuprofen as site I and site II probes, respectively. Laser flash photolysis of **1** at $\lambda_{exc} = 355$ nm in PBS/air gave rise to several transient species; by contrast, in the presence of 1 equiv of proteins, only the triplet excited state was detected. Moreover, the triplet lifetime (τ_T) monitored at 420 nm lengthened considerably (up to 50-fold) in the protein media. This can be attributed to a slower deactivation of the species inside the protein binding pockets, where an exceptional microenvironment provides protection from attack by a second molecule of **1**, oxygen, or other reagents. In agreement with the results from fluorescence titration, the presence of two binding sites in SAs was revealed by two different triplet lifetimes; by contrast, only one τ_T value was found for HAAG and BAAG. The major, longer-lived component under nonsaturating conditions was assigned to $(\mathbf{1}@SA)_{II}$, while the minor component was assigned to $(\mathbf{1}@SA)_I$. Irradiation of **1** at 350 nm in PBS/air led to anthraquinone as a major product. In the presence of proteins, the degree of conversion was markedly lower than in PBS, as revealed by the photodegradation kinetics monitored through the absorbance changes at 367 nm. Thus, a dramatic protection from photooxidation is provided within the protein microenvironment.

Introduction

Proteins play a crucial role in the relevant processes of living organisms. Transport proteins, such as serum albumin or α-acid glycloproteins, are carriers of endogenous or exogenous agents, including drugs or metabolites, in the bloodstream. Human (HSA) and bovine (BSA) serum albumins have a well-known primary structure and similar folding. The former consists of a single chain of 585 amino acid residues containing 17 disulfide bridges, one tryptophan (Trp), and one free cysteine.[1] Small organic molecules bind primarily to two high-affinity sites in HSA, called site I (warfarin binding site) and site II (indole-benzodiazepine binding site), with association constants in the range of 10^4-10^6 M^{-1}.[2] Likewise, BSA is one of the most frequently used proteins in biochemical research; BSA and HSA present 76% sequence identity, but the former contains two Trp residues, instead of one. In general, the structural differences observed between these albumins are mainly of a conservative nature. A number of studies on the drug−protein binding process have used BSA as a model, due to its similarity to HSA.[3] However, the binding behavior of several ligands (naproxen, carprofen, and ibuprofen, among others) to the bovine protein has been proven to be different from that found for the human protein.[4]

α-Acid glycoproteins (AAGs) are one of the major types of acute phase proteins. Their serum concentration increases in response to a systemic tissue injury, inflammation, or infection. Human AAG (HAAG) consists of one polypeptide chain with 183 amino acids, two disulfide bridges, and a molecular mass of 44 kDa; it exhibits a high degree of glycosylation, with carbohydrates accounting for ca. 45% of the total mass. Up to seven binding sites have been described for HAAG. However, most drugs and small molecules exclusively bind to one of them, which is large and flexible. Because the other binding sites have much less importance, their role in the transport of substrates is negligible.[5] With respect to bovine AAG (BAAG), binding of some ligands has been studied by fluorescence techniques. The results reveal a basic drug binding site and a steroid hormone binding site, which significantly overlap with each

* To whom correspondence should be addressed. Tel: (+34)963877344. Fax: (+34)963879349. E-mail: mcjimene@qim.upv.es (M.C.J.) or mmiranda@qim.upv.es (M.A.M.).

† On the occasion of a visiting researcher stay in UPV. Present address: Department of Chemistry and Chemical Biology, Graduate School of Engineering, Gunma University, Kiryu, Gunma 376-8515, Japan.

10.1021/jp104900r © 2010 American Chemical Society
Published on Web 08/09/2010

CHART 1

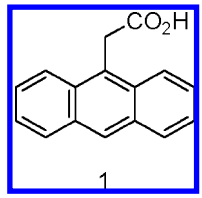

other, but do not contain a specific acidic ligand binding region. The hydrophobic nature of the binding pockets on the two AAGs is similar, while their microviscosities are markedly different.

Because of their ability to bind a number of ligands, proteins can be envisaged as microvessels, where the photoreactivy of included hosts can be modified due to conformational restrictions in the binding pockets, protection against external factors, chirality induced by the amino acid residues, etc. Thus, some examples of modified photoreactivity of target molecules within protein pockets have been reported in the past decade, including dehalogenation, dimerization, cyclization, or isomerization.[6]

The main photochemical pathways for anthracene derivatives are dimerization and oxidation.[7] In the case of 9-substituted anthracenes, regioselective control of photocycloaddition in organic solvents and within confined media has been reported.[8] Moreover, stereoselective photodimerization of 2-anthracenecarboxylate within serum albumins at low protein/substrate ratios has been investigated by Inoue's group.[9]

Herein, we report a detailed study on the photochemistry and photophysics of the anthracene chromophore within proteins, under nonsaturating conditions. Specifically, we have selected 9-anthraceneacetic acid (**1**) (Chart 1) as a simple, water-compatible derivative of this chromophore, with special emphasis on the changes produced upon binding to serum albumins and AAGs.

Experimental Section

Materials and Solvents. HSA, BSA, HAAG, BAAG, anthracene, and acetic anhydride were purchased from Sigma-Aldrich. Potassium permanganate was from Scharlau. Phosphate-buffered saline (PBS) solution (pH 7.4, 0.01 M) was prepared by dissolving Sigma tablets in the appropriate amount of deionized water. All of the solvents were high-performance liquid chromatography (HPLC) quality.

Experimental Procedure for the Synthesis of 9-Anthraceneacetic Acid (1). Compound **1** was obtained following a reported procedure.[10] Thus, to a refluxing suspension of 5.00 g of anthracene (28 mmol) in 30 mL of acetic anhydride, 1.11 g of $KMnO_4$ (7 mmol) was added during 1 h. After the described work up, **1** was obtained as a yellow solid. Its chemical structure was unambiguously confirmed by ^1H NMR.

Absorption Measurements. Optical spectra in different solvents were measured on a Perkin-Elmer Lambda 35 UV/vis spectrometer.

Fluorescence Measurements. Emission spectra were recorded on an Edinburgh FS900 spectrofluorometer system, provided with a M300 monochromator in the wavelength range of 200−900 nm. Samples were placed into 10 × 10 mm^2 Suprasil quartz cells with a septum cap. Solutions were purged with nitrogen or oxygen for at least 15 min before measurements. Fluorescence quantum yields were determined using anthracene as the standard ($\phi_F = 0.27$ at 366 nm in ethanol).[11] The absorbance of the samples at the excitation wavelength was kept below 0.2. Excitation and emission slits were maintained unchanged during the emission experiments. For time-resolved fluorescence decay measurements, the conventional single photon counting technique was used.

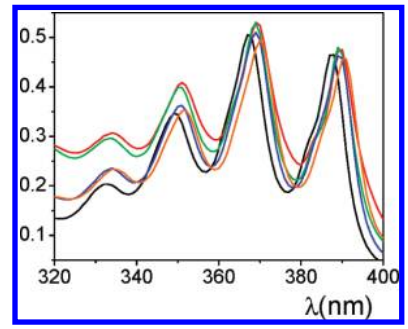

Figure 1. UV−vis spectra of **1** at a 0.11 mM concentration in PBS (black) and in the presence of different proteins at a 1:1 molar ratio: HSA (red), BSA (green), HAAG (blue), and BAAG (orange).

Displacement Experiments. To a solution containing **1** (5 μM) and HSA (10 μM) in PBS, increasing amounts of warfarin or ibuprofen were added (from 0 to 50 μM). Then, the fluorescence intensity at 414 nm was recorded for every sample.

Laser Flash Photolysis (LFP). LFP experiments were performed by using a Q-switched Nd:YAG laser (Quantel Brilliant, 355 nm, 15 mJ per pulse, 5 ns fwhm) coupled to a mLFP-111 Luzchem miniaturized equipment. This transient absorption spectrometer includes a ceramic xenon light source, 125 mm monochromator, Tektronix 9-bit digitizer TDS-3000 series with 300 MHz bandwidth, compact photomultiplier and power supply, cell holder and fiber optic connectors, fiber optic sensor for laser-sensing pretrigger signal, computer interfaces, and a software package developed in the LabVIEW environment from National Instruments. The LFP equipment supplies 5 V trigger pulses with programmable frequency and delay. The rise time of the detector/digitizer is ~3 ns up to 300 MHz (2.5 GHz sampling). The monitoring beam is provided by a ceramic xenon lamp and delivered through fiber optic cables. The laser pulse is probed by a fiber that synchronizes the LFP system with the digitizer operating in the pretrigger mode. All transient spectra were recorded employing 10 × 10 mm^2 quartz cells with 4 mL capacity. The laser spot diameter in the cuvette was ca. 4 mm. The absorbance of **1** was ca. 0.2 at the laser excitation wavelength (355 nm), corresponding to a concentration of 7.5 × 10^{-5} M. All of the experiments were carried out in PBS (pH 7.4, 0.01 M) at room temperature and under air atmosphere.

Displacement Experiments. To **1**/protein equilibrated solutions, the indicated amounts of oleic acid or ibuprofen were added; then, solutions were kept in the dark for 30 min, and decay traces at 420 nm were registered.

General Irradiation Procedure. Solutions of **1** (0.1 mM, $A_{366} = 0.5$) in PBS (with and without protein) were irradiated for 2 h through pyrex inside a Luzchem multilamp photoreactor, with the light from two 8 W lamps (Hitachi FL8BL-B) emitting mainly at 350 nm. The course of the reaction was followed by UV−vis spectroscopy.

Results and Discussion

Absorption Properties. The UV−vis absorption spectrum of **1** exhibited four maxima between 320 and 400 nm. In the presence of proteins, these maxima were red-shifted (Figure 1), whereas the molar absorption coefficients (ε) slightly decrease. These minor changes suggested the formation of complexes (**1**@protein) between **1** and proteins.

The stoichiometry for **1**@protein formation was investigated by means of the corresponding Job plots,[12] where the absorbance

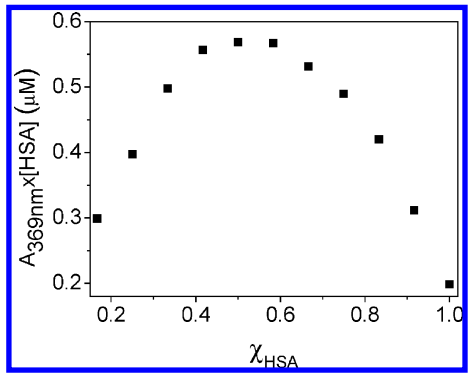

Figure 2. UV absorption Job plot for **1**/HSA at a total concentration of 0.6 mM.

of **1**/protein mixtures was represented as a function of the protein molar fraction. In all cases, a maximum at $\chi_{protein} = 0.5$ was observed, indicating the formation of 1:1 complexes. As an example, the Job plot obtained for HSA is shown in Figure 2. For the other proteins (BSA, HAAG, and BAAG), see Figure S1 in the Supporting Information.

Emission Studies. The fluorescence spectrum of **1** in PBS consisted of a structured emission with maxima between 390 and 470 nm. The addition of increasing amounts of HSA resulted in a decrease of the emission intensity (Figure 3A). In the presence of BSA (Figure 3B), HAAG, or BAAG, the same trend was observed, although the changes were less pronounced.

Fluorescence quantum yields [Φ_F (**1**)] were obtained at λ_{exc} = 367 nm in all media, using anthracene as a standard [Φ_F(s) = 0.27 in ethanol] and eq 1:[13]

$$\Phi_F(\mathbf{1}) = \frac{a_\mathbf{1}}{a_S} \times \frac{A_S}{A_\mathbf{1}} \times \frac{n_{PBS}^{\ 2}}{n_{EtOH}^{\ 2}} \times \Phi_F(s) \qquad (1)$$

where a_S and $a_\mathbf{1}$ are the areas of emission spectra (integration between 375 and 550 nm), n_{PBS} and n_{EtOH} are the refractive indexes, and A_1 and A_S are the absorbances. The $\Phi_F(\mathbf{1})$ values decreased in the presence of equimolar amounts of proteins. The results are shown in Table 1.

The singlet energy was obtained from the intersection between excitation (λ_{em} = 414 nm) and emission bands (λ_{exc} = 366 nm), after normalization. Very similar values were obtained in all media (Table 1).

Fluorescence lifetimes of **1** [$\tau_F(\mathbf{1})$] in air-equilibrated solutions (ca. 10.5 ns) were found to be independent of the presence of protein. The corresponding fluorescence constant values, $k_F(\mathbf{1})$, were obtained from eq 2:

TABLE 1: Singlet Excited State Properties of 1 in PBS, Alone, and in the Presence of Proteins at a 1:1 Molar Ratio

protein	$\Phi_F(\mathbf{1})^a$	E_s (kcal/mol)	k_F (**1**) ($\times 10^{-7}$ s^{-1})^a
none	0.42	72.9	4.3
HSA	0.27	72.5	2.9
BSA	0.36	72.5	3.6
HAAG	0.34	72.9	3.1
BAAG	0.38	72.9	3.5

[a] Relative errors lower than 5% of the stated values.

$$k_F(\mathbf{1}) = \frac{\Phi_F(\mathbf{1})}{\tau_F(\mathbf{1})} \qquad (2)$$

Determination of binding constants was achieved from fluorescence titration, considering the possibility of one or two binding sites. Thus, in the case of reversible binding to the protein (P) involving only one site (eq 3), where K_B is the binding constant and K_D represents the dissociation constant)

$$\mathbf{1} + P \underset{K_D}{\overset{K_B}{\rightleftharpoons}} \mathbf{1}@P \qquad (3)$$

changes of the observed fluorescence intensity (F) of a mixture would be given by eq 4,[14] where a and b are proportionality constants and F_0 is the initial fluorescence intensity.

$$\frac{F}{F_0} = a[\mathbf{1}] + b[\mathbf{1}@P] \qquad (4)$$

Also taking into account the mass balance (eqs 5 and 6) in the equilibrium constant for the dissociation process (eq 7), the concentration of the complex **1**@P is a function of $[\mathbf{1}]_0$, $[P]_0$, and K_B.

$$[\mathbf{1}] = [\mathbf{1}]_0 - [\mathbf{1}@P] \qquad (5)$$

$$[P] = [P]_0 - [\mathbf{1}@P] \qquad (6)$$

$$K_B = \frac{[\mathbf{1}@P]}{[\mathbf{1}][P]} \qquad (7)$$

Experiments were performed keeping $[\mathbf{1}]_0$ constant and varying $[P]_0$ between 0 and 1.4 μM. Mathematical analysis of F/F_0 data (shown in Figure 4 for HAAG and BAAG) in terms the set of eqs 4−7, using a nonlinear least-squares algorithm,[15] allowed us to obtain K_B values of (2.31 ± 0.06) × 10^6 M^{-1} for

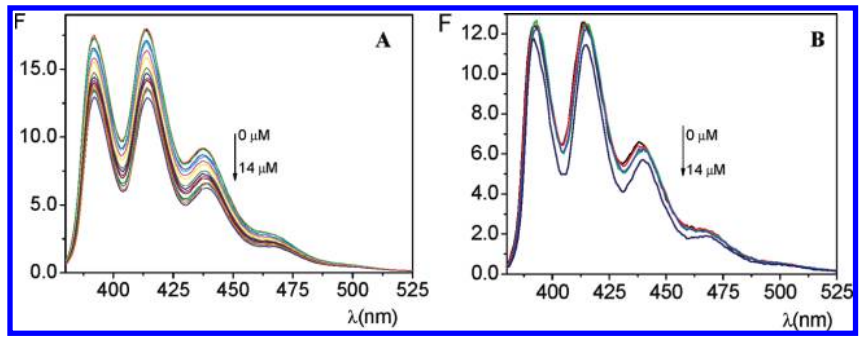

Figure 3. Emission spectra of **1** (2.8 μM in PBS) upon addition of increasing amounts of (A) HSA and (B) BSA (0−14 μM).

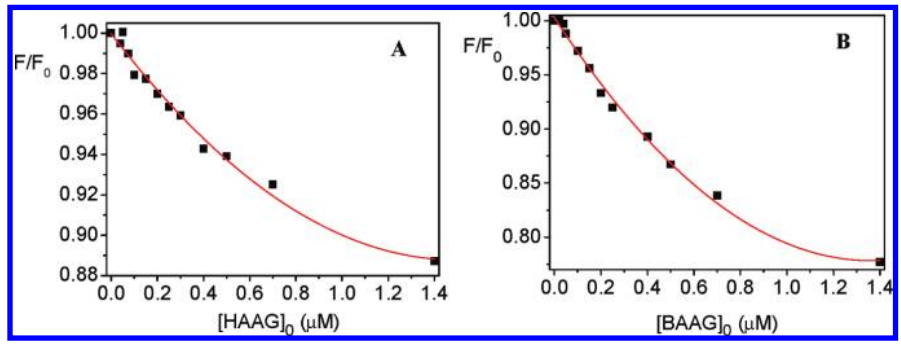

Figure 4. Changes in the relative fluorescence intensity (F/F_0) of **1** plotted against protein concentration, together with the fit to one binding site. (A) HAAG and (B) BAAG.

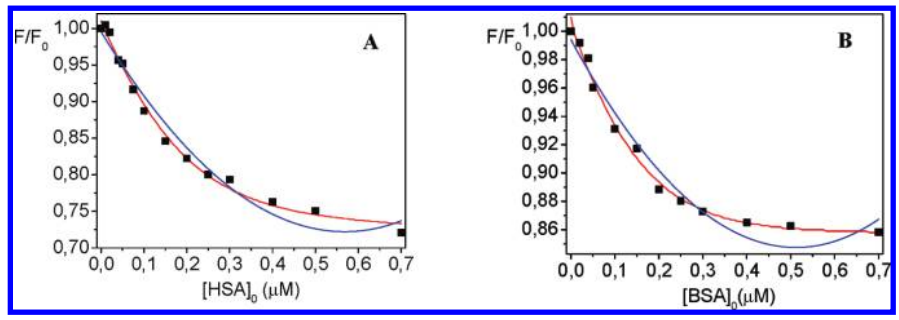

Figure 5. Changes in the relative fluorescence intensity (F/F_0) of **1** plotted against protein concentration, together with the fit to one (blue) or two (red) binding sites. (A) HSA and (B) BSA.

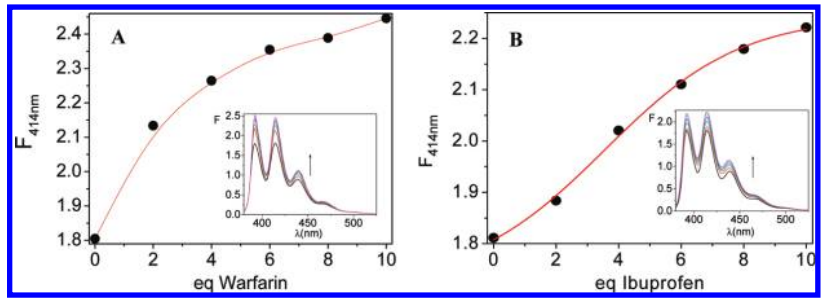

Figure 6. Changes at $\lambda_{em} = 414$ nm of a mixture of **1** (5 μM) and HSA (10 μM), upon addition of increasing amounts (0−50 μM) of (A) warfarin and (B) ibuprofen. Insets: Full emission spectra under the same conditions.

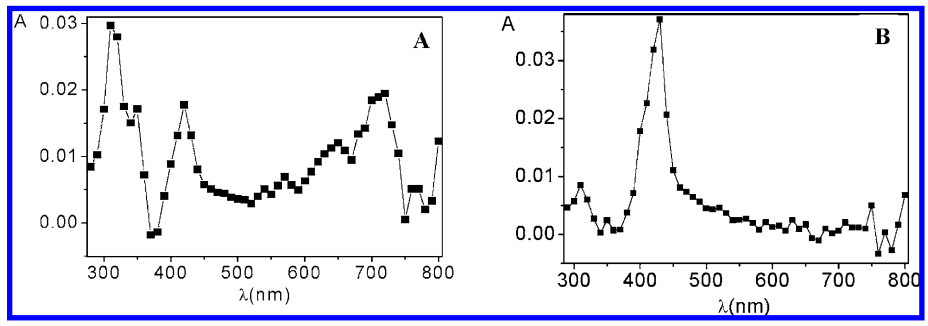

Figure 7. Transient absorption spectra for **1** at 355 nm recorded 2.9 μs after laser pulse in (A) PBS and (B) the presence of HSA (1:1 molar ratio).

binding to HAAG and (2.39 ± 0.05) × 10^6 M^{-1} for BAAG, with a R^2 value equal to 0.995.

In the case of HSA and BSA, the fit of the experimental data following this procedure was not fully satisfactory ($R^2 = 0.974$). This can be related to the fact that HSA and BSA have two different binding pockets, site I and site II.[2] The former is larger, and its main interactions with ligands are hydrophobic in nature, whereas in site II, hydrogen bonding and electrostatic forces predominate.[1] Thus, the possibility of two binding constants for the equilibria represented in eq 8 was considered.

$$(\mathbf{1}@\mathrm{P})_{II} \underset{K_{B_{II}}}{\overset{K_{D_{II}}}{\rightleftharpoons}} \mathbf{1} + \mathrm{P} \underset{K_{D_I}}{\overset{K_{B_I}}{\rightleftharpoons}} (\mathbf{1}@\mathrm{P})_I \qquad (8)$$

The observed fluorescence intensity (F) of a mixture would be given by eq 9,[15] where a, b, and c are proportionality constants and F_0 is the initial fluorescence intensity.

$$\frac{F}{F_0} = a[\mathbf{1}] + b[\mathbf{1}@\mathrm{P}]_I + c[\mathbf{1}@\mathrm{P}]_{II} \qquad (9)$$

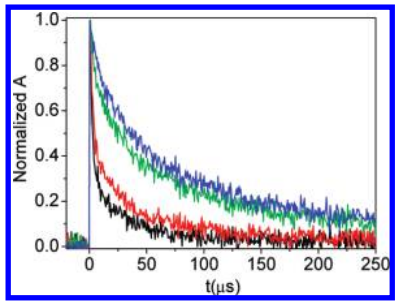

Figure 8. Decays monitored at 420 nm after excitation of **1** at 355 nm in PBS (black) and in the presence of HSA 1:0.1 (red), 1:0.5 (green), and 1:1 (blue) molar ratios.

TABLE 2: Triplet Excited State Lifetimes of 1 (A_{355} = 0.2) in Aerated PBS and within Proteins at a 1:1 Molar Ratio

protein	τ_T (μs)
none	2
HSA	20,[a] 85[b]
BSA	28,[a] 99[b]
HAAG	36
BAAG	36

[a] Minor component. [b] Major component.

Also taking into account the mass balance (eqs 10 and 11), in the equilibrium constant for the dissociation process (eqs 12 and 13)

$$[\mathbf{1}] = [\mathbf{1}]_0 - [\mathbf{1}@\mathrm{P}]_\mathrm{I} - [\mathbf{1}@\mathrm{P}]_\mathrm{II} \quad (10)$$

$$[\mathrm{P}] = [\mathrm{P}]_0 - [\mathbf{1}@\mathrm{P}]_\mathrm{I} + [\mathbf{1}@\mathrm{P}]_\mathrm{II} \quad (11)$$

$$K_{\mathrm{B_I}} = \frac{[\mathbf{1}@\mathrm{P}]_\mathrm{I}}{[\mathbf{1}][\mathrm{P}]} \quad (12)$$

$$K_{\mathrm{B_{II}}} = \frac{[\mathbf{1}@\mathrm{P}]_\mathrm{II}}{[\mathbf{1}][\mathrm{P}]} \quad (13)$$

Mathematical treatment of F/F_0 data (shown in Figure 5 for HSA and BSA) using eqs 10−13 and again a nonlinear least-squares algorithm[14b] allowed us to obtain for HSA $K_{\mathrm{B_I}} = (4.57 \pm 0.08) \times 10^4\ \mathrm{M}^{-1}$ and $K_{\mathrm{B_{II}}} = (1.45 \pm 0.03) \times 10^6\ \mathrm{M}^{-1}$. For BSA, $K_{\mathrm{B_I}}$ and $K_{\mathrm{B_{II}}}$ were found to be $(1.44 \pm 0.03) \times 10^4$ and $(1.20 \pm 0.02) \times 10^6\ \mathrm{M}^{-1}$, respectively.

Binding within two different sites of SAs for **1** was confirmed by displacement experiments using warfarin and ibuprofen as site I and site II probes, respectively.[16] Thus, solutions of **1** (5 μM in PBS) in the presence of either HSA or BSA (10 μM in PBS) were titrated with increasing concentrations of the displacement probes (up to 50 μM). A significant increase of the fluorescence intensity was observed with both warfarin and ibuprofen (see Figure 6 for HSA and Figure S2 in the Supporting Information for BSA), which is in agreement with the two-sites model.

SCHEME 1: Irradiation of 1 in PBS under Aerobic Conditions

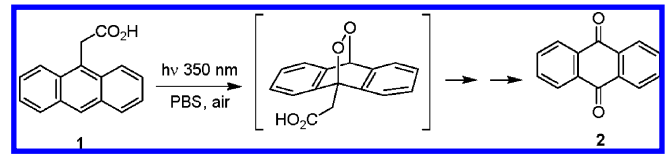

Transient Absorption Spectroscopy. The transient spectrum obtained for **1** upon LFP at λ_{exc} = 355 nm in aerated PBS is shown in Figure 7A. Several transient species were detected under these conditions. On the basis of the literature data, they could be ascribed to the benzylic type radical (λ_{abs} = 310 nm),[17] the radical anion (λ_{abs} = 350 and 420 nm),[18] the triplet excited state (λ_{abs} = 420 nm),[19] the radical cation (λ_{abs} = 600−750 nm),[20] and the hydrated electron (λ_{abs} = 700 nm, only observable within the first microsecond). However, a dramatic change was observed in the presence of 1 equiv of proteins. In all cases, the triplet excited state was the only transient species detected (see Figure 7B for **1**@HSA and Figure S3 in the Supporting Information for **1**@BSA, **1**@HAAG, and **1**@BAAG).

It is also noticeable that the triplet lifetime (τ_T) monitored at 420 nm lengthened considerably in the protein media (see Figure 8 for HSA and Table 2). Figures S4 and S5 in the Supporting Information show the results for the other proteins. This can be attributed to a slower deactivation of the species inside the protein binding pockets, where an exceptional microenvironment provides protection from attack by a second molecule of **1**, oxygen, or other reagents, as well as from triplet−triplet annihilation.[21] Again, the presence of two binding sites in serum albumins was revealed by two different triplet lifetimes. In contrast, only one τ_T value was found for HAAG and BAAG, which can be correlated with the presence of only one binding site in these proteins.

Moreover, LFP experiments were performed in the presence of oleic acid[22,23] or (*S*)-ibuprofen[21d,24] as displacement probes for site I or II, respectively. Thus, the addition of both probes resulted in a significant shortening of the decay traces, associated with the appearance of free **1** (Figure 9).

It is well established that α-aryl-substituted carboxylic acids bind preferentially to site II of serum albumins.[25] Hence, the major component under nonsaturating conditions (τ_T = 85 or 99 μs) was assigned to $(\mathbf{1}@\mathrm{SA})_\mathrm{II}$, while the minor component (τ_T = 20 μs or 28) was assigned to $(\mathbf{1}@\mathrm{SA})_\mathrm{I}$.

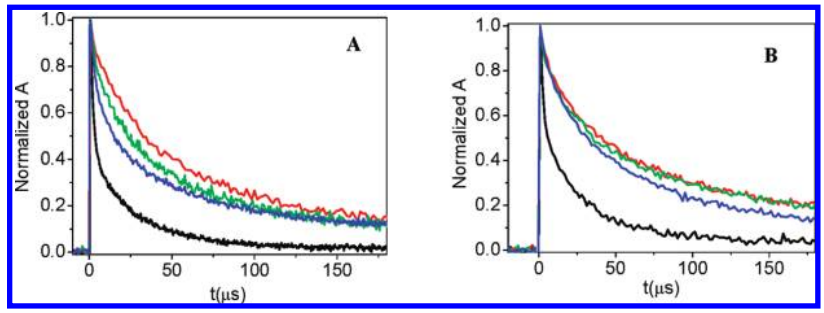

Figure 9. Decays monitored at 420 nm after excitation of **1** at 355 nm in PBS (black), **1**/SA 1:1 molar ratio (red), **1**/SA/ibuprofen 1:1:1 molar ratio (green), and **1**/SA/oleic acid 1:1:1 molar ratio (blue). (A) For HSA and (B) for BSA.

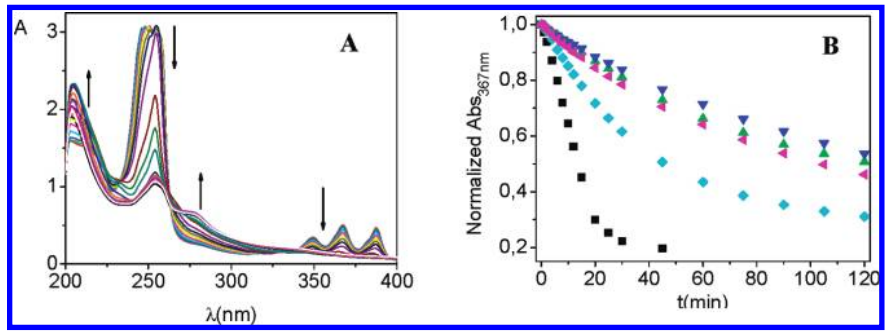

Figure 10. (A) UV−vis spectra of a solution of **1** in PBS after UV irradiation at different times (0−120 min). (B) Kinetics (normalized data of A_{397}) for the photodegradation process of **1** in aerated PBS solution (black square) and within HSA (green triangle), BSA (blue inverted triangle), HAAG (aqua diamond), and BAAG (pink triangle).

TABLE 3: Rate Constants (k_r) for the Photooxidation of 1 in Different Media

protein	k_r ($\times 10^{-4}$ min^{-1})
none	14.0
HSA	1.55
BSA	1.33
HAAG	4.24
BAAG	2.02

Steady-State Photolysis in the Presence of Proteins. Irradiation of **1** at 350 nm in aerated PBS afforded anthraquinone (**2**) as the major product. This can be explained by quenching of the triplet excited state of **1** by oxygen, with the formation of $^1O_2$. Formal [4 + 2] cycloaddition of the latter to the central anthracene ring, followed by rearrangement of the resulting endoperoxide and loss of acetic acid, would lead to the observed product (Scheme 1).[26] Similar photooxidation processes have been reported for the parent anthracene.[7d−h]

The photoreaction was monitored by UV absorption spectroscopy (Figure 10A), following the decrease of the resolved long-wavelength band pattern characteristic of the anthracene chromophore. Irradiation of **1** was also performed in the presence of SAs or AAGs at a 1:1 molar ratio (see Figure S6 in the Supporting Information). Under these experimental conditions, the formation of anthracene dimers was prevented, since the probability of two molecules of **1** sharing the same protein pocket is negligible. In the presence of proteins, anthraquinone was also the only detected photoproduct. However, the degree of conversion was markedly lower than in PBS. A dramatic protection from photooxidation was provided within the protein microenvironent in all cases, as revealed by the photodegradation kinetics, monitored through the absorbance changes at 367 nm (Figure 10B). First-order fitting of the kinetic traces led to the rate constants shown in Table 3. Hence, data show that a protective effect was especially remarkable for HSA, BSA, and BAAG.

Conclusions

It has been shown that 9-anthraceneacetic acid is a simple and water-compatible probe, suitable for photophysical and photochemical studies on the anthracene chromophore in homogeneous and microheterogeneous media. This chromophore exhibits a remarkable enhanced photostability when located inside proteins, where a unique microenvironment is available that provides protection of the excited states from the attack by oxygen or other reagents. The results from steady-state irradiations correlate well with the absence of radical ionic species in transient absorption spectroscopy and also with the dramatically longer (up to 50-fold) triplet lifetimes within the protein binding sites. This is a structure-specific effect, as demonstrated by the significant differences found between serum albumins and AAGs of different species.

Acknowledgment. Financial support from the MEC (Grant CTQ2007-67010) and from the Generalitat Valenciana (Prometeo Program, ref 2008/090) is gratefully acknowledged.

Supporting Information Available: Figures of Job plot diagrams for **1**, fluorescence experiments with displacement probes for **1**, LFP spectra for **1**, decays of the signal at 420 nm, decays and fittings for the signal at 420 nm, and changes in the absorption spectra of **1**. This material is available free of charge via the Internet at http://pubs.acs.org.

References and Notes

(1) (a) Peters, T. *All About Albumins: Biochemistry, Genetics and Medical Applications*; Academic Press: San Diego, 1995. (b) He, X. M.; Carter, D. C. *Nature* **1992**, *358*, 209.

(2) Sudlow, G.; Birkett, D. J.; Wade, D. N. *Mol. Pharmacol.* **1975**, *11*, 824.

(3) (a) Li, B. X.; Zhang, Z. J.; Zhao, L. X. *Anal. Chim. Acta* **2002**, *468*, 65. (b) Kwing, T. C. *Clin. Chim. Acta* **1985**, *151*, 193. (c) Svenson, C. K.; Woodruff, M. N.; Baxter, J. G.; Lalka, D. *Clin. Pharmacokinet.* **1985**, *11*, 450.

(4) (a) Wei, S.; Zhao, L.; Cheng, X.; Lin, J.-M. *Anal. Chim. Acta* **2005**, *545*, 65. (b) Kitamura, K.; Kume, M.; Yamamoto, M.; Takegami, S.; Kitade, T. *J. Pharm. Biomed. Anal.* **2004**, *36*, 411. (c) Silva, D.; Cortez, C.; Louro, S. R. W. *Spectrochim. Acta, Part A* **2004**, *60*, 1215. (d) Gelamo, E. L. C.; Silva, H. T. P.; Imasato, H.; Tabak, M. *Biochim. Biophys. Acta* **2002**, *1594*, 84. (e) Sulkowska, A. *J. Mol. Struct.* **2002**, *614*, 227. (f) Kuchimanchi, K. R.; Ahmed, M. S.; Johnston, T. P.; Mitra, A. K. *J. Pharm. Sci.* **2001**, *90*, 659. (g) Gelamo, E. L.; Tabak, M. *Spectrochim. Acta, Part A* **2000**, *56*, 2255. (h) Fleury, F.; Kudelina, I.; Nabiew, I. *FEBS Lett.* **1997**, *406*, 151. (i) Sun, P.; Hoops, A.; Hartwick, R. A. *J. Chromatogr. B* **1994**, *661*, 335. (j) Kohita, H.; Matsushita, Y.; Moriguchi, I. *Chem. Pharm. Bull.* **1994**, *42*, 937. (k) Valsami, G. N.; Panayotis, M.; Koupparis, M. A. *Pharm. Res.* **1991**, *8*, 888. (l) Whitlam, J. B.; Crooks, M. J.; Brown, K. F.; Pedersen, P. V. *Biochem. Pharmacol.* **1979**, *28*, 675. (m) Muller, W. E.; Wollert, U. *Biochem. Pharmacol.* **1976**, *25*, 141.

(5) (a) Kopecky, V., Jr.; Ettrich, R.; Hofbauerova, K.; Baumruk, V. *Biochem. Biophys. Res. Commun.* **2003**, *300*, 41. (b) Rojo-Dominguez, A.; Hernandez-Arana, A. *Protein Seq. Data Anal.* **1993**, *5*, 349. (c) Schmid, K.; Nimberg, R. B.; Kimura, A.; Yamaguchi, H.; Binette, J. P. *Biochim. Biophys. Acta* **1977**, *492*, 291. (d) Aubert, J. P.; Loucheux-Lefebvre, M. H. *Arch. Biochem. Biophys.* **1976**, *175*, 400. (e) Schmid, K.; Kaufman, H.; Isemura, S.; Bauer, F.; Emura, J.; Motoyama, T.; Ishiguro, M.; Nanno, S. *Biochemistry* **1973**, *12*, 2711. (f) Schmid, K. *J. Am. Chem. Soc.* **1953**, *75*, 60.

(6) (a) Ouchi, A.; Zandomeneghi, G.; Zandomeneghi, M. *Chirality* **2002**, *14*, 1–11. (b) Lhiaubet-Vallet, V.; Sarabia, Z.; Bosca, F.; Miranda, M. A. *J. Am. Chem. Soc.* **2004**, *126*, 9538–9539. (c) Lhiaubet-Vallet, V.; Bosca, F.; Miranda, M. A. *J. Phys. Chem. B* **2007**, *111*, 423–431.

(7) (a) Bouas-Laurent, H.; Castellan, A.; Desvergne, J.-P.; Lapouyade, R. *Chem. Soc. Rev.* **2001**, *30*, 248. (b) Bouas-Laurent, H.; Castellan, A.; Desvergne, J.-P.; Lapouyade, R. *Chem. Soc. Rev.* **2000**, *29*, 43. (c)

Becker, H. D. *Chem. Rev.* **1993**, *93*, 145. (d) Guarini, A.; Tundo, P. *J. Org. Chem.* **1987**, *52*, 3501. (e) Aspler, J.; Carlsson, D. J.; Wiles, D. M. *Macromolecules* **1976**, *9*, 691. (f) Sugiyama, N.; Iwata, M.; Yoshioka, M.; Yamada, K.; Aoyama, H. *Chem. Commun.* **1968**, 1563. (g) Voyatzakis, E.; Jannakoudakis, D.; Dorfmiiller, T.; Sipitanos, C. *Compt. Rend.* **1959**, *249*, 1756. (h) Dufraisse, C.; Gerard, M. *Bull. Soc. Chim. France* **1937**, *4*, 2052.

(8) (a) Wu, D.-Y.; Chen, B.; Fu, X.-G.; Wu, L.-Z.; Zhang, L.-P.; Tung, C.-H. *Org. Lett.* **2003**, *5*, 1075. (b) Wu, D.-Y.; Zhang, L.-P.; Wu, L.-Z.; Wang, B.-J.; Tung, C.-H. *Tetrahedron Lett.* **2002**, *43*, 1281. (c) Tung, C.-H.; Guan, J.-Q. *J. Org. Chem.* **1998**, *63*, 5857.

(9) (a) Pace, T. C. S.; Nishijima, M.; Wada, T.; Inoue, Y.; Bohne, C. *J. Phys. Chem. B* **2009**, *113*, 10445. (b) Nishijima, M.; Wada, T.; Mori, T.; Pace, T. C. S.; Bohne, C.; Inoue, Y. *J. Am. Chem. Soc.* **2007**, *129*, 3478. (c) Nishijima, M.; Pace, T. C. S.; Nakamura, A.; Mori, T.; Wada, T.; Bohne, C.; Inoue, Y. *J. Org. Chem.* **2007**, *72*, 2707. (d) Wada, T.; Nishijima, M.; Fujisawa, T.; Sugahara, N.; Mori, T.; Nakamura, A.; Inoue, Y. *J. Am. Chem. Soc.* **2003**, *125*, 7492.

(10) Galanin, N. E.; Yakubov, L. A.; Shaposhnikov, G. P. *Russ. J. Gen. Chem.* **2007**, *77*, 1448.

(11) Murov, S. L.; Carmichael, I.; Hug, G. L. *Handbook of Photochemistry*; Marcel Dekker: New York, 1993.

(12) (a) Huang, C. Y. *Methods Enzymol.* **1982**, *87*, 509. (b) Job, P. *Ann. Chim.* **1928**, *9*, 113.

(13) Lakowicz, J. R. *Principles of Fluorescence Spectroscopy*; Springer Science+Business Media: New York, 2006.

(14) (a) Epps, D. E.; Raub, T. J.; Kezdy, F. *J. Anal. Biochem* **1995**, *227*, 342. (b) Bisson, A. P.; Hunter, C. A.; Morales, J. C.; Young, K. *Chem.—Eur. J.* **1998**, *4*, 845.

(15) (a) Epps, D. E.; Raub, T. J.; Kezdy, F. *J. Anal. Biochem* **1995**, *227*, 342. (b) Bisson, A. P.; Hunter, C. A.; Morales, J. C.; Young, K. *Chem.—Eur. J.* **1998**, *4*, 845.

(16) (a) Fehske, K. J.; Müller, K. J.; Schläfer, U.; Wollert, U. *Prog. Drug Protein Binding* **1981**, *2*, 5. (b) Itoh, T.; Saura, Y.; Tsuda, Y.; Yamada, H. *Chirality* **1997**, *9*, 643.

(17) Meiggs, T. O.; Grossweiner, L. I.; Miller, S. I. *J. Am. Chem. Soc.* **1972**, *94*, 7981.

(18) Fukuzumi, S.; Ohkubo, K.; Imahori, H.; Guldi, D. M. *Chem.—Eur. J.* **2003**, *9*, 1585.

(19) Bensasson, R.; Land, E. J. *Trans. Faraday Soc.* **1971**, *67*, 1904.

(20) Scaiano, J. C.; Nguyen, K.-T. *Can. J. Chem.* **1982**, *60*, 2286.

(21) (a) Pérez-Ruiz, R.; Bueno, C. J.; Jiménez, M. C.; Miranda, M. A. *J. Phys. Chem. Lett.* **2010**, *1*, 829. (b) Bueno, C. J.; Jiménez, M. C.; Miranda, M. A. *J. Phys. Chem. B* **2009**, *113*, 6861. (c) Vayá, I.; Bueno, C. J.; Jiménez, M. C.; Miranda, M. A. *Chem.—Eur. J.* **2008**, *14*, 11284. (d) Vayá, I.; Bueno, C. J.; Jiménez, M. C.; Miranda, M. A. *ChemMedChem* **2006**, *1*, 1015. (e) Jiménez, M. C.; Miranda, M. A.; Vayá, I. *J. Am. Chem. Soc.* **2005**, *127*, 10134.

(22) Montanaro, S.; Lhiaubet-Vallet, V.; Jimenez, M. C.; Blanca, M.; Miranda, M. A. *ChemMedChem* **2009**, *4*, 1196.

(23) Petitpas, I.; Gruène, T.; Bhattacharya, A. A.; Curry, S. *J. Mol. Biol.* **2001**, *314*, 955.

(24) Kohita, H.; Matsushita, Y.; Moriguchi, I. *Chem. Pharm. Bull.* **1994**, *42*, 937.

(25) Lapicque, F.; Muller, N.; Payan, E.; Dubois, N. *Clin. Pharmacokinet.* **1993**, *25*, 115.

(26) Gilbert, A.; Baggot, J. *Essentials of Molecular Photochemistry*; Blackwell Scientific Publications: Oxford, 1991.

JP104900R